

2-DIMENSIONAL REGULARIZATION FOR THE RETRIEVAL OF PROFILES OF MICROPHYSICAL AEROSOL PROPERTIES FROM MULTIWAVELENGTH RAMAN LIDAR

Alexei Kolgotin,⁽¹⁾ Detlef Müller⁽²⁾

⁽¹⁾Physics Instrumentation Center, Troitsk, Moscow Region, 142190, Russia, E-mail: alexeift@yahoo.com

⁽²⁾Leibniz Institute for Tropospheric Research, Permoserstr. 15, 04318 Leipzig, Germany, E-mail: detlef@tropos.de

ABSTRACT

Microphysical parameters, e.g., effective radius and complex refractive index of atmospheric particles are derived from measurements of volume backscatter and extinction coefficients with the method of inversion with regularization. In the classic approach the optical data of individual height layers of the profiles are treated separately in the inversion procedure. We propose an extension of this technique by simultaneously inverting optical data sets of successive height layers. This approach still is in a highly exploratory status, but bears several advantages over the technique used so far. Preliminary results from simulations with synthetic data show that the uncertainties of the derived particle microphysical properties can be reduced. Accordingly the single scattering-albedo, which describes particle absorption, can be retrieved with higher accuracy. Considering optical data sets of several height layers simultaneously in the inversion is the first true approach to retrieving profiles of microphysical properties of aerosol particles.

1. ONE-DIMENSIONAL PROBLEM: "RADIUS"-DIRECTION

In order to understand the 2-dimensional regularization approach, we start with outlining the classical 1-dimensional regularization technique. For that we consider individual height layers, and solve the resulting Fredholm integral equations of the first kind for the investigated particle size distribution:

$$\int_{r_{\min}}^{r_{\max}} K(m, \lambda_l, r) f(r) dr = g(\lambda_l), \quad l = \overline{1, N_w} \quad (1)$$

The term $g(\lambda_l)$, describes the extinction and backscatter coefficients at wavelength λ_l . The index l denotes the number N_w of particle backscatter and extinction coefficients. The particle size distribution is written as $f(r)$. We assume spherical particle shape. The Mie-efficiency [1] kernels are written as $K(m, \lambda_l, r)$. Here r_{\min} and r_{\max} denote the lower and the upper limits of the particle

radii considered in the inversion. The parameter m is the complex refractive index.

In order to solve the set of integral equations one approximates the distribution $f(r)$ by a superposition of base functions $B_i(r)$:

$$f(r) \approx \sum_{i=1}^{N_B} c_i B_i(r), \quad i = \overline{1, N_B} \quad (2)$$

The index i describes the number of base functions N_B used for reconstructing the investigated particle size distribution. The so-called weight coefficients c_i , which have to be determined in the inversion, are found by rewriting Eqs. (1) and (2) into a set of linear equations [3]:

$$\mathbf{A}\mathbf{c}=\mathbf{g}. \quad (3)$$

The elements of the kernel matrix \mathbf{A} are written as:

$$A_{li} = \int_{r_{\min}}^{r_{\max}} K(m, \lambda_l, r) B_i(r) dr \quad (4)$$

The optical data are expressed by the optical data vector \mathbf{g} .

The simple solution of Eq. (3), i.e., $\mathbf{c} = \mathbf{A}^{-1}\mathbf{g}$ leads to unphysical solutions (ill-posed inverse problem). One has to introduce constraints, such as smoothness of the investigated particle size distribution in order to stabilize the inverse problem. This step is called regularization. A detailed description of how this is done for the problem described here can be found in [3,4]. The final solution for the weight vector is written as:

$$\mathbf{c} = (\mathbf{A}^T \mathbf{A} + \gamma \mathbf{H})^{-1} \mathbf{A}^T \mathbf{g} \quad (5)$$

The matrix \mathbf{H} contains the prescribed smoothness conditions. The Lagrange multiplier γ determines the strength of smoothing. The term \mathbf{A}^T is the transposed matrix of the kernel matrix \mathbf{A} .

2. ONE-DIMENSIONAL PROBLEM: “REFORMULATED”

The lidar measurements deliver optical data for different height layers. Therefore Eqs. (1) and (3) are re-written for the different height layers:

$$\int_{r_{\min}^{(j)}}^{r_{\max}^{(j)}} K(m^{(j)}, \lambda_l, r) f^{(j)}(r) dr = g^{(j)}(\lambda), \quad j = 1 \dots N_L \quad (6)$$

$$\mathbf{A}^{(j)} \mathbf{c}^{(j)} = \mathbf{g}^{(j)} \quad (7)$$

The index j now describes the N_L height layers.

This set of linear equations (7) can be expressed in terms of a vector-matrix relationship, i.e.,

$$\mathbf{J}\mathbf{C} = \mathbf{G} \quad (8)$$

Similarly to the steps leading from Eq. (3) to the regularized Eq. (4) one can also re-formulate Eq. (8) into the following expression, which describes the regularization step:

$$\mathbf{C} = (\mathbf{J}^T \mathbf{J} + \gamma \mathbf{H})^{-1} \mathbf{J}^T \mathbf{G}. \quad (9)$$

The matrices \mathbf{J} and \mathbf{H} , and the vectors \mathbf{C} and \mathbf{G} have the following structures:

$$\mathbf{J} = \begin{bmatrix} [\mathbf{A}^{(1)}]_{N_w \times N_B} & \mathbf{O} & \dots & \mathbf{O} \\ \mathbf{O} & [\mathbf{A}^{(2)}]_{N_w \times N_B} & \dots & \mathbf{O} \\ \dots & \dots & \dots & \mathbf{O} \\ \mathbf{O} & \mathbf{O} & \dots & [\mathbf{A}^{(N_L)}]_{N_w \times N_B} \end{bmatrix}_{N_L N_w \times N_B N_L},$$

$$\mathbf{H} = \begin{bmatrix} [\mathbf{H}^{(1)}]_{N_B \times N_B} & \mathbf{O} & \dots & \mathbf{O} \\ \mathbf{O} & [\mathbf{H}^{(2)}]_{N_B \times N_B} & \dots & \mathbf{O} \\ \dots & \dots & \dots & \dots \\ \mathbf{O} & \mathbf{O} & \dots & [\mathbf{H}^{(N_L)}]_{N_B \times N_B} \end{bmatrix}_{N_B N_L \times N_B N_L},$$

$$\mathbf{C} = \left([\mathbf{c}^{(1)}]_{N_B \times 1} \mid [\mathbf{c}^{(2)}]_{N_B \times 1} \mid \dots \mid [\mathbf{c}^{(N_L)}]_{N_B \times 1} \right)_{N_B N_L \times 1}^T,$$

$$\mathbf{G} = \left([\mathbf{g}^{(1)}]_{N_w \times 1} \mid [\mathbf{g}^{(2)}]_{N_w \times 1} \mid \dots \mid [\mathbf{g}^{(N_L)}]_{N_w \times 1} \right)_{N_L N_w \times 1}^T$$

The solutions for the weight vector $\mathbf{c}^{(j)}$ in the different height layers $j = \overline{1, N_L}$ (Eq. (9)), are independent from each other. Now we introduce the new step, i.e., we

assume a smoothing condition along the height z with the help of another matrix $\tilde{\mathbf{H}}$. In this way we link successive height layers, which is a reasonable physical constraint, because particle physical properties in different height layer normally will not vary drastically, but rather gradually when going from one height layer to the next layer.

3. TWO-DIMENSIONAL PROBLEM: “HEIGHT” - DIRECTION

The aerosol properties along the z -direction are described by the following functions:

$$\begin{aligned} K(m^{(j)}, \lambda, r) &\rightarrow K(m(z), \lambda, r), & f^{(j)}(r) &\rightarrow f(z, r), \\ g^{(j)}(\lambda) &\rightarrow g(z, \lambda), & c^{(j)} &\rightarrow c(z) \end{aligned} \quad (10)$$

Integrating Eq. (1) over $z \in [z_{\min}, z_{\max}]$ leads to the classic two-dimensional Fredholm integral equation of the first kind:

$$\int_{z_{\min}}^{z_{\max}} \int_{r_{\min}}^{r_{\max}} K(m(z), \lambda_l, r) f(z, r) dr dz = \tilde{g}(\lambda_l), \quad (11)$$

where

$$\tilde{g}(\lambda_l) = \int_{z_{\min}}^{z_{\max}} g(z, \lambda_l) dz. \quad (12)$$

Substituting again the approximation (2) for the investigated particle size distribution into Eq. (11) gives:

$$\sum_{i=1}^{N_B} \int_{z_{\min}}^{z_{\max}} \tilde{K}_i(m(z), \lambda_l) c_i(z) dz = \tilde{g}(\lambda_l) \quad (13)$$

The function $\tilde{K}_i(m(z), \lambda_l)$ is defined by the right-hand side of expression (4). The sum in Eq. (13) can be split by using the factors φ_i , $\sum_{i=1}^{N_B} \varphi_i = 1$, so that

$$\int_{z_{\min}}^{z_{\max}} \tilde{K}_i(m(z), \lambda_l) c_i(z) dz = \varphi_i \tilde{g}(\lambda_l) \quad i = \overline{1, N_B} \quad (14)$$

Eq. (14) again describes a set of Fredholm integral equations of the first kind, but now along the z direction in analogy to the set of equations (6). In this case the extended linear equations system

$$\tilde{\mathbf{I}}\tilde{\mathbf{C}} = \tilde{\mathbf{G}} \quad (15)$$

can again be solved by inversion with regularization:

$$\tilde{\mathbf{C}} = (\mathbf{I}^T \mathbf{I} + \chi \mathbf{H})^{-1} \mathbf{I}^T \tilde{\mathbf{G}} \quad (16)$$

The matrices \mathbf{I} and \mathbf{H} , and the vectors $\tilde{\mathbf{C}}$ and $\tilde{\mathbf{G}}$ have the following structures:

$$\mathbf{I} = \begin{bmatrix} [\mathbf{A}_1]_{N_w \times N_L} & \mathbf{O} & \dots & \mathbf{O} \\ \mathbf{O} & [\mathbf{A}_2]_{N_w \times N_L} & \dots & \mathbf{O} \\ \dots & \dots & \dots & \dots \\ \mathbf{O} & \mathbf{O} & \dots & [\mathbf{A}_{N_B}]_{N_w \times N_L} \end{bmatrix}_{N_B N_w \times N_B N_L}$$

$$\mathbf{H} = \begin{bmatrix} [\mathbf{H}_1]_{N_L \times N_L} & \mathbf{O} & \dots & \mathbf{O} \\ \mathbf{O} & [\mathbf{H}_2]_{N_L \times N_L} & \dots & \mathbf{O} \\ \dots & \dots & \dots & \dots \\ \mathbf{O} & \mathbf{O} & \dots & [\mathbf{H}_{N_B}]_{N_L \times N_L} \end{bmatrix}_{N_B N_L \times N_B N_L}$$

$$\tilde{\mathbf{C}} = \left([\mathbf{c}_1]_{N_L \times 1} \mid [\mathbf{c}_2]_{N_L \times 1} \mid \dots \mid [\mathbf{c}_{N_B}]_{N_L \times 1} \right)_{N_B N_L \times 1}^T$$

$$\tilde{\mathbf{G}} = \left(\varphi_1 [\mathbf{g}]_{N_w \times 1} \mid \varphi_2 [\mathbf{g}]_{N_w \times 1} \mid \dots \mid \varphi_{N_w} [\mathbf{g}]_{N_w \times 1} \right)_{N_B N_w \times 1}^T$$

The vectors \mathbf{c}_i describe the i^{th} weight coefficient in the approximation given by Eq. (2) in direction z .

The vector $\tilde{\mathbf{C}}$ differs from vector \mathbf{C} only by the order of the respective elements (or rows). Reordering the same rows of matrix \mathbf{H} given by Eq. (16), so that vector $\tilde{\mathbf{C}} \rightarrow \mathbf{C}$, allows us constructing the matrix $\tilde{\mathbf{H}}$ fitted for Eq. (9). Finally we thus obtain the two-dimensional regularization approach, presented by

$$\mathbf{C} = (\mathbf{J}^T \mathbf{J} + \gamma \mathbf{H} + \chi \tilde{\mathbf{H}})^{-1} \mathbf{J}^T \mathbf{G} \quad (17)$$

The definition of the regularization parameter γ can be found in [2,4]. For the definition of the regularization parameter χ we suggest the following criterion:

$$\sum_{j=1}^{N_L} |c_1^{(j)}(\chi)| \rightarrow \min_{\chi \in [0, \infty]} \quad (18)$$

4. SIMULATION EXAMPLE

We briefly show an example for the 2-dimensional regularization, expressed by Eq. (17), and compare the results obtained with Eq. (9). This work still is in a very exploratory phase, and our first concern is to test, if the

results of the one-dimensional regularization can be reproduced by the two-dimensional regularization.

Fig. 1 shows a simple profile of microphysical parameters (solid lines) on the basis of an aerosol size distribution $f(r)$ with mean radius $r_{mean} = 0.1 \mu\text{m}$, geometrical standard deviation 0.41, and variable number concentration. We assumed three particle layers. For the lower layer we chose $N_{t1} = 1 \text{ cm}^{-3}$, for the second layer we chose $N_{t2} = 0.5 \text{ cm}^{-3}$, and for the topmost layer we chose $N_{t3} = 0.01 \text{ cm}^{-3}$. The layers had equal geometrical depth of 1600 m. The upper layer basically has to be regarded as the background case. For theoretical reasons it is not possible to set the layer to zero particle concentration.

As a further simplification we assume a height independent complex refractive index with real part $\text{Re}(m)=1.45$, and imaginary part $\text{Im}(m)=0.005$. These two parameters were assumed to be known in the following inversion.

Fig. 2 shows the profiles of optical data generated from the microphysical parameters with a Mie-scattering code [1]. Particle backscatter coefficients $\beta(\lambda)$ were calculated for the wavelengths at 355, 532, and 1064 nm, and extinction coefficients $\alpha(\lambda)$ were calculated at 355 and 532 nm. For each layer we generated several data points, as indicated by the symbols. Statistical noise of up to 10% was applied to the optical profiles. The synthetic profiles of the optical data were then processed by means of Eqs. (9) and (17) and compared.

In the case of Eq. (9) the optical data were analyzed for the different layers individually according to the de-

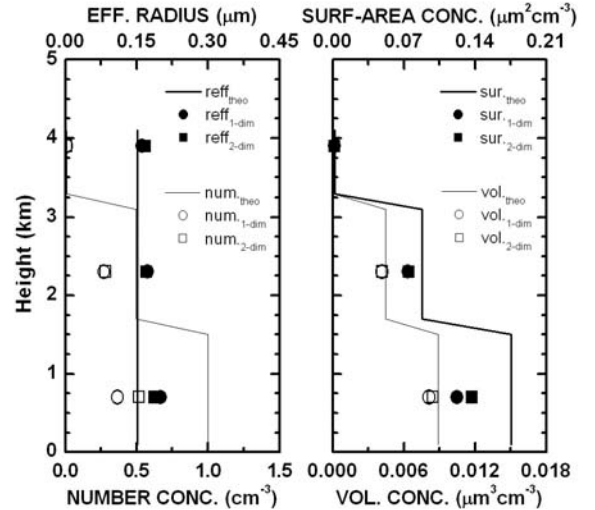


Fig. 1: (left) Profile of number concentration (thin line), and value of effective radius (thick line) in the three particle layers chosen for the simulations. The uppermost layer was chosen such that it describes background conditions. The symbols denote the results from the inversion for the 1-dimensional and the 2-dimensional regularization. (right) Results are shown for surface-area and volume concentration.

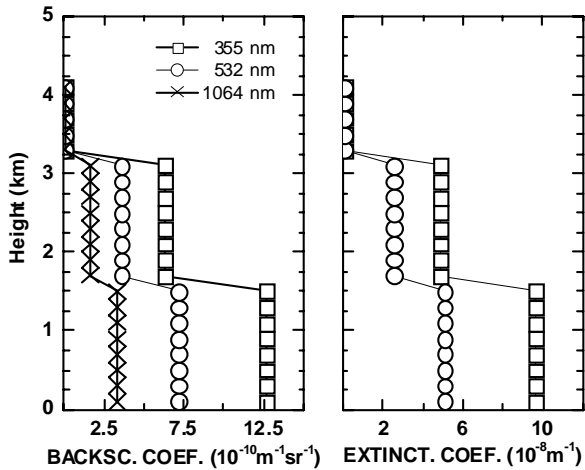


Fig.2 (left) Profile of particle backscatter coefficient at the three measurement wavelengths used for the inversion. The symbols denote that several “measurement” points were assumed for each particle layer. (right) Profiles of the particle extinction coefficients for the two measurements wavelengths used for the inversion.

descriptions given by [2, 4]. In the case of Eq. (17) we analyzed all three particle layers simultaneously, whereby the smoothing matrix $\tilde{\mathbf{H}}$ was set to unity in a first approximation. Quite clearly future work will be to identify a more appropriate choice of $\tilde{\mathbf{H}}$. In the regularization we considered 260 inversion windows [3]. The lower integration limit r_{\min} was set from 0.03 μm to 0.15 μm with a stepwidth of 0.01 μm . The upper integration limits r_{\max} was set from 0.25 μm to 5 μm with a stepwidth of 0.25 μm .

Fig. 1 displays the mean results and the resulting uncertainties. The different symbols denote the findings for the case of the 1-dimensional and the 2-dimensional inversion for the three particle layers, respectively. In that respect we analyzed the results corresponding to the center of the layers. Most importantly one sees comparably good agreement for the two approaches. As mentioned before, the main intention of the first feasibility studies is to show that this extended scheme of 2-dimensional regularization is applicable at all.

In general we find uncertainties that have already been noted for the 1-dimensional case, i.e. particle effective radius is estimated with uncertainties of $\leq 30\%$, volume and surface-area concentration in general can be estimated with uncertainties of $\leq 50\%$, whereas number concentration often exhibits errors of 50-100%. In fact, Fig. 1 even shows a slight improvement regarding the accuracy of the derived parameters, even though the smoothing matrix $\tilde{\mathbf{H}}$, which will be of critical importance in the forthcoming simulation studies, has not been chosen well.

5. CONCLUSIONS

Two-dimensional regularization is a new approach to the inversion of profiles of optical data into microphysical particle properties. This method makes explicit use of the profile information delivered by multiwavelength aerosol Raman lidar. The underlying mathematical problem belongs to the class of so-called ill-posed inverse problems, i.e., solutions in general are not unique with respect to the input data, solutions are highly sensitive to measurement errors and require a minimum amount of input information. Some of these difficulties can be overcome by regularization, i.e., mathematical and physical constraints are used to stabilize the inversion process. This approach however does not allow for a straightforward retrieval of particle properties for the case of 1-dimensional regularization which considers optical data in individual height layers. False results may still occur, and consequently very time consuming post-processing of inversion results is required.

First simulations have shown that the errors of the derived microphysical particle parameters can be reduced with the 2-dimensional regularization. Post-processing of inversion results can be reduced as well. It seems possible to better handle and exploit the information content of large data sets acquired by multiwavelength Raman lidars organized in lidar networks like the European Aerosol Research Lidar Network. This approach may offer a key to incorporating optical profiles from space-borne lidar (CALIPSO) and/or airborne lidar (e.g. the Langley Airborne HSRL system) in the analysis of data from ground-based lidar stations.

It should be emphasized though that this work presented here still is in a very preliminary status. Detailed simulation studies will be needed to assess the potential of this new technique.

REFERENCES

1. Bohren C. F. and Huffman D. R., *Absorption and Scattering of Light by Small Particles*, John Wiley, Hoboken, New Jersey, 1983.
2. Müller D., et al., Microphysical Particle Parameters From Extinction and Backscatter Lidar Data by Inversion With Regularization: Theory, *Appl. Opt.*, Vol. 38, 2346 – 2357, 1999.
3. Twomey S, *Introduction to the Mathematics of Inversion in Remote Sensing and Indirect Measurements*, Elsevier, Amsterdam, The Netherlands, 1977.
4. Veselovskii, I. et al., Inversion With Regularization for the Retrieval of Tropospheric Aerosol Parameters From Multiwavelength Lidar Sounding, *Appl. Opt.*, Vol. 41, 3685 – 3699, 2002.